Radioactive ^{55}Fe Contamination in the Primary Circuit of WWER-440

T. Ruskov[1], R. Ruskov[1], I. Dobrevski[1], P. Menut[2], S. Konnova[1], N. Zaharieva[1]

[1] Institute for Nuclear Research and Nuclear Energy, Bulgarian Academy of Sciences, Sofia, Bulgaria
[2] International Atomic Energy Agency, Vienna, Austria

1. Introduction

The isotope ^{55}Fe is generated in the steel construction materials of the reactor mainly by the reaction ^{54}Fe (n,γ) ^{55}Fe. In natural isotope abundance ^{54}Fe is 5.81%. The thermal neutron capture cross-section of this reaction is 3.25*b*. Thus, enormous radioactivity of ^{55}Fe (T1/2=2.73*y*) will take place in the reactor construction materials after several years operation [1].

Due to corrosion processes and iron-bearing corrosion-products (crud) transport in the primary water system of the reactor a radioactive ^{55}Fe contamination will take place on the inner walls of the primary circuit as well.

The decay scheme of ^{55}Fe is shown in Figure 1 [2]. Due to pure electron capture decay of ^{55}Fe, only X-rays ($K\alpha$=5.9 keV and $K\beta$=6.49 keV) and Auger electrons with energy 5.19 keV are emitted. The range of this radiation in the matter depends on the average Z and density of the sample. For human tissue this range is: 5 mm for X-rays and about 3000 Å for Auger electrons [3,4]. Thus, the ^{55}Fe isotope is not so dangerous in the case of external irradiation but dangerous at the internal irradiation by the following reasons:

- It is known that almost 70% of the total human body iron is bound in the haemoglobin. The rest is stored in other constituents of the blood;
- The biological half-life of Fe (removal from hole body) is 5.48 *y* [5];
- Thus, at the internal irradiation, due to inhalation of aerosols or oral intake by gastrointestinal tract one could expect the radiation damage in the blood constituents or marrow, increasing the leukaemia risk;
- The very small range of ^{55}Fe radiation makes difficult the check of the intake activity in particular with conventional dosimeter instruments.

That is why, permanent ^{55}Fe control in the NPP is desired. Unfortunately, up to the present such control has not been done everywhere. It should be emphasized that particularly in the case of decommissioning of nuclear power plants the ^{55}Fe control is obligatory.

Two mechanisms for generation of the ^{55}Fe are of importance:

The direct generation of the ^{55}Fe due to the neutron irradiation of the different iron-contained parts of the reactor system such as the steel shell of the reactor core, the core basket, the steel shaft, the reactor vessel and others.

The direct generation of ^{55}Fe was calculated using the specially developed programme code DIRGEN [1].

Another type of contamination, considered in this paper is due to the corrosion of materials and erosion-dissolution processes in the primary circuit of WWER with their subsequent deposition-precipitation on the inner surface of the primary circuit. The real time calculations of the ^{55}Fe activity are performed by means of the updated computer code MIGA-RT, (K. Dinov, et al. [6]). These calculations include the distribution of ^{55}Fe activity between the reactor coolant and the primary circuit surfaces, including core, steam generator tubing, hot and cold main circulation loops, and cleanup system.

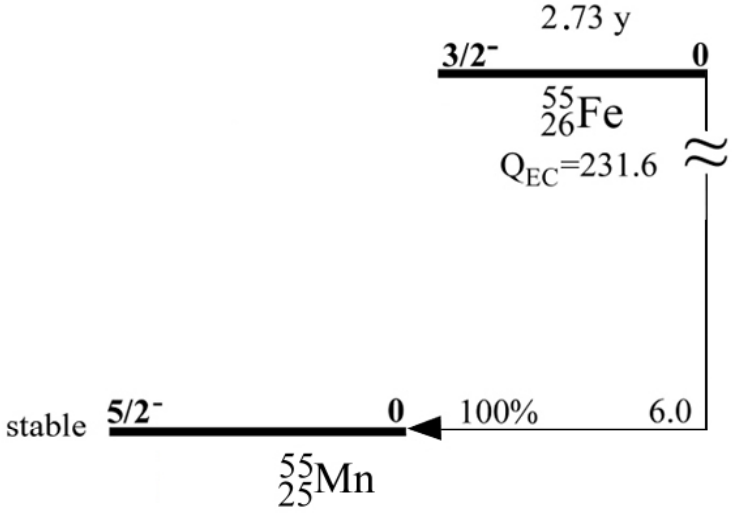

Figure 1. Decay scheme of ^{55}Fe

2. Mathematical Description of the Radioactive Corrosion Products Generation and Their Transport in the Primary Circuit System

We have used the properly updated programme code MIGA-RT [6,7,8] for real time calculations in order to take into account the generation of ^{55}Fe and its deposition on the surface of different reactor nodes.

It should be noted that the code MIGA-RT was successfully used to describe the contamination of the primary circuit of the WWER-440 type reactors like Slovakian EBO-1, Finland LOVIISA-1,2, and also the French reactor CRUAS-1 as for the isotopes ^{58}Co and ^{60}Co [8]. It was shown to be in a good agreement both with other computer codes aiming the same purposes and the experiment – all provided during an international benchmark guided by IAEA.

With some modifications the programme code MIGA-RT was adapted to calculate ^{55}Fe in the corrosion product deposition on the inner surface of different reactor nodes. Bellow, we shall make a brief sketch of the main features of the programme code MIGA.

The main processes in the primary circuit of WWER-440 that influences the activity buildup at the system components and the activity of the coolant are shortly described bellow:

1. Corrosion of component materials and forming the inner and outer oxides layers at the circuit surfaces.
2. Release of the oxides (corrosion products – CP) into the coolant by erosion or dissolution.
3. Growing of the crud by precipitation or deposition of the CP from the coolant; The CP in the coolant are supposed to be dissolved or in a particulate form. In the real case also different colloidal pre-forms may exist.
4. Activation of the CP in the coolant and those deposited on the reactor surfaces under irradiation. Due to a permanent mixing process as for the reactor coolant, the model operates with an average (on the reactor core) neutron fluxes.

A test of this model was successfully performed using the operating experience of WWER-440 (PAKS NPP, Units 1&2, Hungary), WWER-1000 (Kozloduy NPP, Units 5&6, Bulgaria, Beznau PWR NPP [7]).

In the implemented physico-chemical approach for the model, iron plays the main role. Thus, one may expect that the MIGA code as a whole should be capable to explain the activity data for ^{55}Fe/^{59}Fe equally well as for ^{58}Co/^{60}Co.

An example of the mass-activity transport equations implemented into the MIGA-RT code is given bellow. For the total content of the *i*-th parent element in the coolant (m_i) we can write (1):

$$\frac{dm_i}{dt} = \sum_{j=1}^{n} k_{ij}^{1} m_{ij}^{w} - \sum_{j=1}^{n} \frac{4}{d_j^h} k_{ij}^{d} m_i^p \beta_j - \tag{1}$$

$$- \sum_{j=1}^{n} k_{ij}^{dp} F_j \rho_j \left(C_{ij}^c - S_{ij}^w\right) - m_i(\eta) + c_t \sum_{j=1}^{n} \sum_{k=1}^{m} f_i^k F_j^k$$

For the total deposition of the *i*-th element on the surface of the *j*-th node (m_{ij}^W) we can write (2):

$$\frac{dm_{ij}^w}{dt} = \frac{4}{d_j^h} k_{ij}^d m_i^p \beta_j - k_{ij}^l m_{ij}^w + k_{ij}^{dp} F_j \rho_j (C_{ij}^c - S_{ij}^w) \tag{2}$$

The deposition on the CVCS node (the cleanup system) (m_i^{CVCS}) is described by the Equation (3):

$$\frac{dm_i^{CVCS}}{dt} = \eta_i^p m_i^p + \eta_i^s m_i^s \tag{3}$$

Analogous equations can be written for the total deposition of the *i*-th radionuclide: in the coolant (m_i^*), on the surface of the *j*-th node ($m_{ij}^{w^*}$), and in the CVCS node ($m_i^{CVCS^*}$). One should add to the terms in the above equations a term reflecting the radioactive decay like: $-m_i^* \lambda_i$ and terms corresponding to the generation of the *i*-th radionuclide in the coolant and on the surfaces under direct neutron irradiation into the reactor core (for more details see Dinov, et al. [8]). A symbol description of the Eqs. (1), (2) and (3) is given bellow in Table 1.

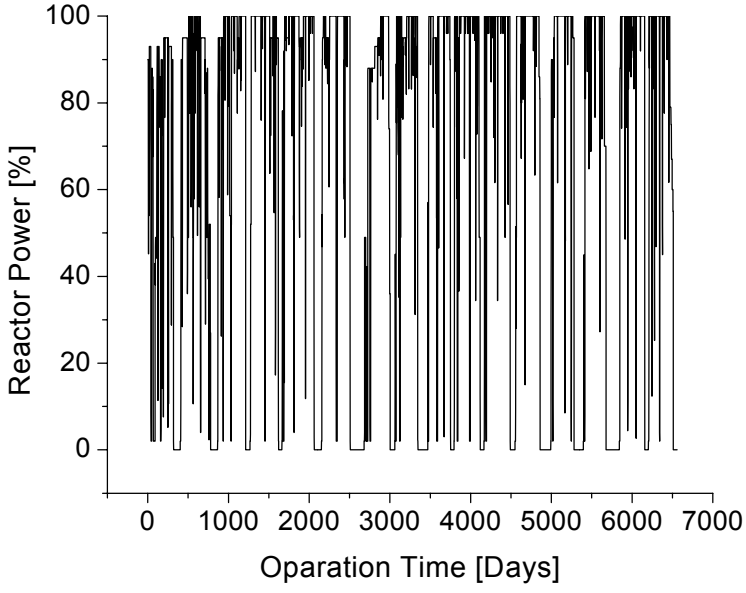

Figure 2. Power history of EBO-1 Unit

As an example a calculation of the deposited ^{55}Fe crud activity using real time data concerning the reactor power and physico-chemical conditions for the first 16 cycles of Slovakian reactor EBO-1 was performed. The "power history" of the reactor is presented in Figure 2.

We have performed calculations of the ^{55}Fe activity deposited as a crud on the walls of different reactor nodes and also in the reactor coolant. We have considered at this stage up to 5 nodes as follows: the reactor core, the steam generator tubing, hot and cold main circulation loops (called shortly hot and cold legs), and the cleanup system.

A part of the input data is presented in Table 2 that characterizes the WWER-440 system. It should be emphasized that in these types of reactor systems the same austenitic stainless steel (SS) (08Cr18Ni10T) was used as a construction material for the reactor, steam generator tubing, and hot and cold legs.

Another important part of the input data, which we did not present in this table concerns the real time data for the reactor power and for the physico-chemical conditions. A daily average of the relevant characteristics is undertaken. The physico-chemical conditions include the boron concentration in the coolant, the concentration of the Li, Na and K ions, concentration of the atomic H, pH data, and some others.

The results for the accumulated activity of the ^{55}Fe isotope at the end of every cycle are given in Table 3. The day history of the activity buildup was calculated as well and presented in Figure 3.

One can see from Table 3 and Figure 3 that the highest ^{55}Fe specific activity deposition appears on the reactor core surface (the fuel ele-

Table 1. General equations symbol description

m_i, m_i^p m_i^s, m_{ij}^w	Deposition of i-th parent element in total, particulate, and soluble form in the coolant, and on the wall of *j*-th node	[nuclei]
m_i^*, $m_i^{p^*}$ $m_i^{s^*}$, $m_{ij}^{w^*}$	Deposition of i-th radionuclide in total, particulate, and soluble form in the coolant, and on the wall of *j*-th node	[nuclei]
k_{ij}^d, k_{ij}^l	Deposition and release coefficients for particulates on the *j*-th node	[m/s]
C_{ij}^c, $C_{ij}^{c^*}$	Concentration of the dissolved parent element and of the radionuclide in the coolant of *j*-th node	[nuclei/kg]
S_{ij}^w, $S_{ij}^{w^*}$	Solubility of the *i*-th parent element and of the daughter radionuclide at the wall area of the *j*-th node	[nuclei/kg]
d_j^h	Hydraulic diameter of *j*-th node	[m]
β_j	Part of the coolant volume of *j*-th node from the total coolant volume	
λ_i	Decay constant of *i*-th isotope	[s^{-1}]
F_j	Effective wetted surface in *j*-th node	[m^2]
ρ_j, ρ_j^ω	Density of water in *j*-th node	[kg/m^3]
η^p, η^s, η^l	Constants of purification of particulates and solubles, leakage constant	[s^{-1}]
R_i, R_{ef}	Net ($\sigma_l\phi$) and effective ($\sigma_l\phi_{ef}$) collision rates of *i*-th radionuclide formation from its parent element	[nuclei/s]
A_i, f_i	Atomic weight of *i*-th parent element and its abundance in the natural isotopes mixture	
N_{av}	Avogadro number	
f_i^k	Content of the *i*-th parent element in the *k*-th material	
F_j^k, F_{co}^k	Wetted surface of the *k*-th material in the *j*-th node	[m^2]

Table 2. Input data

Fuel element cladding surface (Zr – Nb alloy)	3150 m^2
Total primary circuit surface	18850 m^2
Hot leg pipes + Hot collector surface (SS)	160 m^2
Cold leg pipes + Cold collector surface (SS)	177 m^2
Steam generator tubing surface (SS)	12500 m^2
Surface of stainless steel (SS) in core (surface under full irradiation)	960 m^2
Surface of stainless steel out of core	13620 m^2
Coolant volume in the primary system	250 m^3
Nominal power (normalized)	100 %
Temperature at 0 – power and hot stendby	264 °C
Average temperature	279.5 K
Average core thermal neutron flux	$2\cdot10^{13}$ $cm^{-2}s^{-1}$
Average core fast neutron flux	$1.4\cdot10^{14}$ $cm^{-2}s^{-}$]

Table 3. Accumulated ^{55}Fe surface activity at the end of every cycle of the EBO-1 reactor

Cycle №	Operation time days	Refueling time days	Reactor core, [kBq·cm^{-2}]	Hot legs, [kBq·cm^{-2}]	Steam generator tubing, [kBq·cm^{-2}]	Cold legs, [kBq·cm^{-2}]
1	320	82	1770.	77.4	25.1	37.4
2	377	85	2070.	155.	39.4	75.4
3	349	52	2340.	173.	37.8	70.4
4	356	40	2120.	173.	36.3	69.9
5	400	90	1870.	149.	31.1	58.9
6	356	172	1640.	136.	27.7	53.2
7	323	57	1280.	101.	21.3	40.1
8	286	123	1200.	94.	19.7	36.4
9	282	43	1160.	92.6	19.2	35.2
10	326	45	1080.	90.8	19.1	35.7
11	326	60	1160.	95.7	19.4	34.8
12	308	133	1170.	96.7	19.3	34.8
13	289	115	1070.	88.2	17.6	32.5
14	282	164	1070.	86.9	18.0	33.1
15	314	47	1200.	96.6	19.4	34.7
16	308	47	1080.	94.1	19.4	36.0

ment cladding surface). The subsequent procedures with the spent fuel have to take into account eventual ^{55}Fe contamination in different storage places as the spent fuel pool, etc. Indeed, the calculated deposition of ^{55}Fe specific activity on the reactor core surface occurs to be about one order of magnitude more than the calculated deposition of ^{60}Co activity as it is seen in Figure 4. The same relation of the ^{55}Fe and ^{60}Co activities remains valid also for the other primary circuit reactor nodes.

3. Conclusions

1. The control on the isotope ^{55}Fe activity buildup in the reactor systems seems to be very important part of the general radioactivity monitoring during the work of a NPP. It is important especially when some standard repair works are performed in order to prevent possible increase of risk for an internal irradiation.
   The control on the ^{55}Fe isotope distribution in different reactor construction elements and on the surfaces of the primary circuit as a whole becomes much more important and even obligatory when a decommissioning of the reactor system is planned.
2. The ^{55}Fe activity deposition on the inner surfaces of the primary circuits reaches the values of 103 kBq/cm^2 for the reactor core surfaces and 102 kBq.cm^{-2} for the out-of-core surfaces. These activities are an order of magnitude higher than the corresponding activities due to ^{60}Co buildup.
3. In case of an inhalation or ingestion of the crud from the first circuit, where the ^{55}Fe activity is an order of magnitude higher than the ^{60}Co activity, according to the known norms [9], the effective dose (in Sv) obtained from ^{55}Fe and ^{60}Co should be comparable. Moreover, as we mentioned above, the intake of ^{55}Fe is much more dangerous due to possible damages in the blood constituents.
4. The programme code MIGA-RT, updated in this paper can be used also for the reactor systems of WWER-1000 type after proper modification of the input data and some additional calculations.

References

[1] R. Ruskov, T. Ruskov, S. Beloussov, K. Ilieva, T. Apostolov, Iv. Dobrevski, S. Konnova. Generation of ^{55}Fe in the Steel Construction Materials of the WWER Reactor System. International Meeting Nuclear Power in Eastern Europe, Varna, Bulgaria, 17-20 June, 2001.

[2] C. Lederer, V. Shirley. Table of Isotopes, 7-th Ed. Wiley, New York.

[3] E. Storm, H. Israel. Photon Cross Sections from 0.001 to 100 MeV for Elements 1 through 100. Los Alamos Scientific Laboratory, New Mexico, June, 1967.
[4] Alpha-, Beta- and Gamma-ray Spectroscopy. (1), Ed. K. Siegbahn, North-Holland Publ. Co., Amsterdam, 1968.
[5] M. Eisenbud, Environmental Radioactivity From Natural, Industrial and Military Sources. 3-pd Edition, Academic Press, INC., Orlando, San Diego, N.Y., Austin, Boston, London, Sydney, Tokyo, Toronto,1987.
[6] K. Dinov. Modeling of Activity Transport in PWR by Computer Code MIGA. IAEA RCM, Toronto, Canada, 5-9 May, 1997.
[7] H. Venz, K. Dinov. Effect of Primary Water Chemistry on Activity Transport at Unit 2 of Beznau PWR Plant. JAIF 98, Proc. Intern. Conference, Kashiwazaki, Japan, October, 1998.
[8] K. Dinov, Iv. Dobrevsky, N. Zaharieva, P. Menut. Modeling of VVER Light-water Reactors Activity Buildup. Proc. 8-th Intern. Conference on Nuclear Engineering, Baltimore, MD USA, April, 2000.
[9] International Basic Safety Standards for Protection against Ionizing Radiation and for the Safety of Radiation Sources, Safety Series, №115, IAEA, Vienna, 1996.

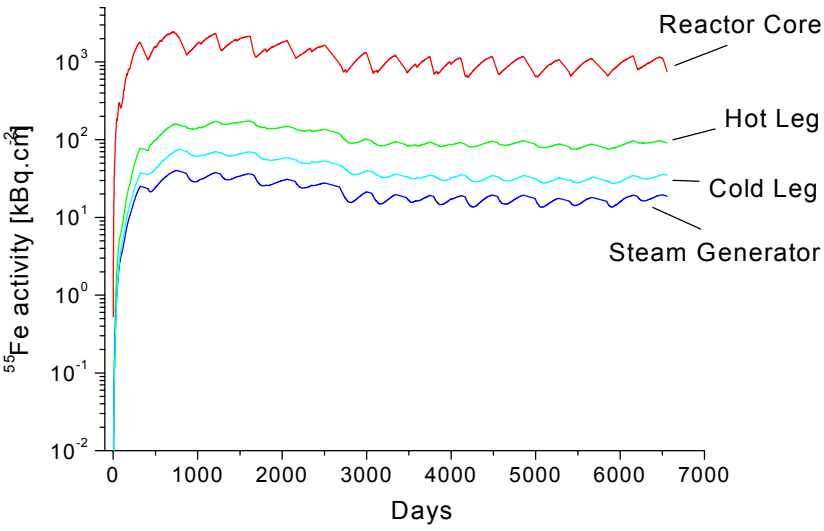

Figure 3. ^{55}Fe activity buildup as a function of time

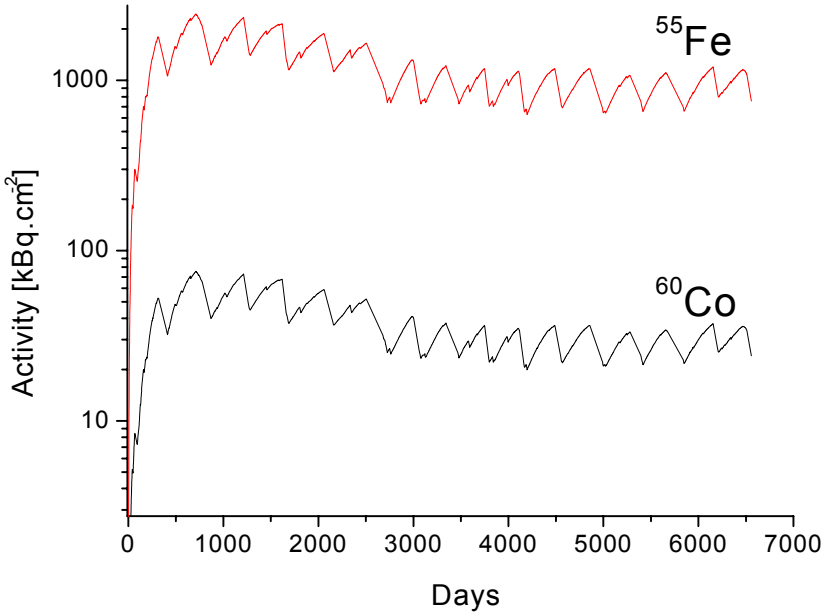

Figure 4. ^{55}Fe vs. ^{60}Co reactor core activity buildup as a function of time